



Cosmetic nanomaterials in the environment: nano-zinc oxide and zinc-influence on soil microorganisms

Elsayed A. Abdelmeged¹ · Gianluca Brunetti² · Waleed H. Shetaya³ · Ezzat R. Marzouk⁴

Received: 9 December 2022 / Accepted: 24 April 2023 / Published online: 15 May 2023
© The Author(s) 2023

Abstract

This study aimed to investigate the impact of water-containing sunblock products with different residual quantities of bulk ZnO or ZnO nanoparticles (NPs) on soil microorganisms using a bioassay toxicity experiment. The two forms of ZnO were studied at different concentrations ranging from 0 to 10 mg L⁻¹, and leachates obtained from the water disposal during a handwashing simulation experiment were also evaluated, along with raw sunblocks containing both bulk ZnO and ZnO NPs (at 50% and 100%). The key characteristics of each type of ZnO material were analyzed using multiple analytical techniques, such as scanning electron microscopy (SEM), transmission electron microscopy (TEM), energy-dispersive X-ray spectroscopy (EDX), X-ray diffraction (XRD), Fourier-transform infrared spectroscopy (FTIR), and ultraviolet–visible spectroscopy (UV–Vis). The outcomes revealed that the stability of ZnO nanoparticles was considerably high, with the highest dissolution rate estimated after 36 h as 0.19% of the sunblock's overall ZnO NPs concentration. The different forms of pure ZnO used in the bacterial bioassay demonstrated that the Zn concentration of 10 mg L⁻¹ exhibited the largest inhibition zone area compared to the other treatments. The disc diffusion bioassay findings confirmed that ZnO NPs are active components with greater toxicity than bulk ZnO. These results demonstrated that the antimicrobial effect was exclusively due to the nano-specific influence at higher concentrations. However, additional research is needed to understand better the environmental effects of different types of ZnO particles disposed of by sunblock users. Examining how such substances react in actual environmental conditions is crucial, as they contain various diverse ingredients that may cause varying reactions compared to bulk ZnO particles.

Keywords ZnO NPs · Sunblock · Soil microorganism · Toxicity

Introduction

Nanomaterials have unique characteristics compared to analog bulk particles (Wu et al. 2022). Their colossal surface area to volume proportion was used to drive new applications or in different technologies for a wide range of functions; in the last decade, they have been commercialized in more than a thousand products in different branches of the global market (Fajardo et al. 2022). Metal oxide nanoparticles (MONPs) became relevant constituents in consumer products such as cosmetics, pharmaceuticals, textiles, solar cells, and paint (McIntyre 2012; Nagarajan 2008; Mboniyivuze et al. 2015; Malhotra and Mandal 2019; Sungur 2021). The environment represents the ultimate sink where these nano-consumer products converge through different discharging pathways such as landfill treatment, wastewater plants, or even air emissions (Hurley and Nizzetto 2018; Pacitto et al. 2021). A key concern is the effect of disposed

✉ Ezzat R. Marzouk
ezzatz_marzouk@aru.edu.eg

- ¹ Geology and Basic Science Department, Institute of Environmental Studies, Arish University, Bir El Abd, North Sinai 45516, Egypt
- ² Science, Technology, Engineering and Mathematics (STEM), Future Industries Institute, University of South Australia, Mawson Lakes, SA 5095, Australia
- ³ Air Pollution Research Department, Environment and Climate Change Research Institute, National Research Centre, 33 El-Bohouth St., Dokki, Giza 12622, Egypt
- ⁴ Soil and Water Department, Faculty of Environmental Agricultural Sciences, Arish University, El-Arish, North Sinai 45516, Egypt

of MONPs on certain bacteria, such as soil microorganisms that play essential roles in a healthy ecosystem food web, including organic waste decomposition and nutrient cycling processes. According to some research in this field, such contaminants could heavily affect the soil microbial community (Liu et al. 2018; Xie et al. 2016; Mayor et al. 2013; Zhao et al. 2021).

It was well established that MONPs show a proven antimicrobial activity against pure bacterial cultures such as *Escherichia coli*, *Bacillus subtilis*, *Streptococcus aureus*, and *Pseudomonas aeruginosa* (Kumar et al. 2013; Hajipour et al. 2012; Madkhali et al. 2021) at a wide range of nanoparticle concentrations starting from 10 up to 5000 mg L⁻¹ (Aruoja et al. 2009; Heinlaan et al. 2008; Santos-Rasera et al. 2022; Gelover et al. 2006). Some previous studies suggest that the toxicity of MONPs to microorganisms is assigned to the disruption of cell membrane activity (Neal 2008; Kubo et al. 2005; Lovrić et al. 2005). Some MONPs, such as TiO₂ NPs, could penetrate the cell membrane through the cytoplasm, destroying the lipid bilayer due to the generation of reactive oxygen species (ROS) in light (Mileyeva-Biebesheimer et al. 2010; Duan et al. 2021). However, even in the absence of light, the toxicity to microorganisms exerted by ROS formation after interaction with MONPs was also identified (Adams et al. 2006; Niazi and Gu 2009).

NPs dissociation behavior producing metal ions has also been reported as a significant element of toxicity to microorganisms (Aruoja et al. 2009). Moreover, the NPs interaction with soil organic matter (SOM) may pose a significant risk to certain soil microorganisms (Neal 2008). For instance, the common NPs tendency to aggregate to themselves and other compounds and their propension to adhere to the microbial cells' surface might also play a significant role in their toxicity (Jiang et al. 2009). However, other studies demonstrated that SOM could promote NPs stability, dispersion, and separation from the surface of bacteria (Li et al. 2010; Neal 2008). Different NPs properties, such as chemical composition, particle size, shape, and surface charge, showed conflicting results concerning the toxicity to microorganisms (Aruoja et al. 2009; Heinlaan et al. 2008; Adams et al. 2006).

This research focused on zinc oxide (ZnO) nanoparticles due to their growing presence in consumer products such as sunblocks. ZnO NPs are employed in these cosmetic products since they behave as UVA (320–400 nm) and UVB (280–320 nm) reflectors because of their high ability to grasp sun radiation. They have also been proven safe for human use, photostable, non-allergenic, and non-irritating when treating human skin (Smijns and Pavel 2011). For these reasons, ZnO NPs are primarily used as an additive in sunblock cream preparations by prestigious international dermo-cosmetic brands (Kołodziejczak-Radzimska and Jesionowski 2014). The main objective of this research was to determine if metal oxide nanoparticles derived from

sunblock-containing ZnO NPs could impact soil microorganisms. The objectives of the current work were to:

- Characterize ZnO nanoparticles obtained from commercial sunblock products.
- Simulate the in-house disposal pathway of ZnO NPs-derived sunblock removed from human skin by a water bath.
- Determine the solubility and dissolution behaviors of ZnO NPs-derived sunblock.
- Evaluate the toxicity of disposed of water containing different residual sunblocks prepared with bulk ZnO or ZnO NPs to soil microorganisms.

Materials and methods

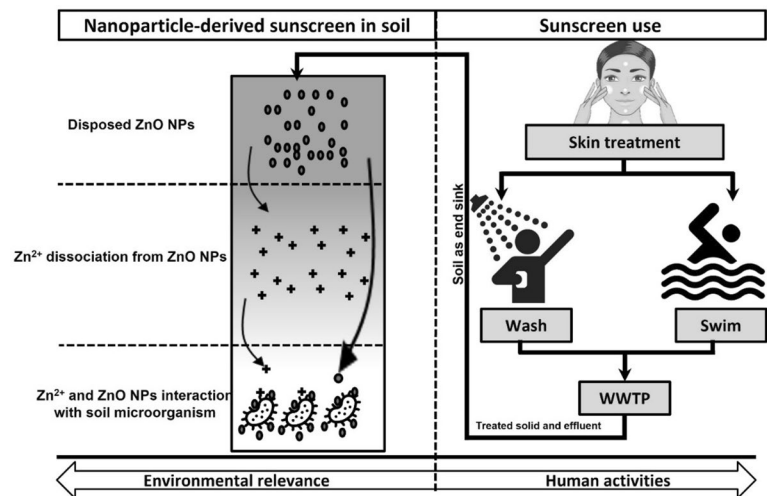
Reagents and commercial sunblock

All chemical substances used were of Trace Analysis Grade (TAG); ultrapure water (18.2 MΩ cm⁻¹ at 25 °C) was used during the dissolution experiment. Zinc oxide nanoparticles (ZnO NPs) were purchased from 'Micronisers Pty Ltd, Australia (line W45/30). According to the manufacturer specification, the ZnO NPs water suspension contained a ZnO concentration of 99.5% w/v, and the average particle size was 40 nm with a specific surface area of 25 m² g⁻¹. Two commercial sunblock creams were purchased from the local market: the first one containing 18% w/v bulk ZnO concentration (Caribbean Sol Sunblock SPF 30 from the USA) and the second containing (18% w/v) nano-size ZnO particles (Bioderma Photoderm Nude Touch Solaire Perfection SPF50, France).

ZnO NP-containing sunblock disposal route simulation

The specific behavior of ZnO NPs sunblocks in municipal greywater disposal has not yet been well addressed. The proposed disposal route of ZnO NP-derived sunblock through a wastewater treatment plant (WWTP) is presented in Fig. 1. A disposal route simulation was performed using four volunteers recruited among postgraduate students and employees of Arish University. A proportion of sunblock cream was spread randomly on each volunteer's hand skin and left for 30 min under laboratory conditions. Each volunteer washed his/her hand continuously in a warm water bath (30 °C) by immersing their hands in the water for 15 min. The supernatant from each test was collected and kept in the dark at 5 °C for future use. The collected supernatant was used to simulate the sunblock released by sunbathers/swimmers after washing/showering in realistic environmental conditions.

Fig. 1 Graphical mechanism for the proposed disposal route of ZnO NPs-derived sunblock



Aliquots of 10 mL from each sample were analyzed for Zn concentrations.

Characterization of tested samples

The samples were sonicated and then prepared to be imaged using a Hitachi-S 3400N SEM (scanning electron microscope with high-energy electrons beam configurable up to 130 kV) (Ibrahim et al. 2022). The presence of elemental Zn was confirmed through an energy dispersive analysis X-ray spectrometer (EDX) coupled with SEM. The samples were also examined using a transmission electron microscope (TEM) operated at an accelerated voltage of 100 kV (JEOL JEM-1000 cx, Japan) (Liu et al. 2009a). The image processing for the particle size analysis was performed by ImageJ software (Ferreira and Rasband 2012).

Zinc oxide content was estimated by a UV–vis spectrophotometer (Hitachi U-3900). For phases identification of all tested samples, it was used a Rigaku Ultima IV X-ray diffractometer (XRD) adopted a Cu K- α radiation at 40 kV and 30 mA, with a 2θ angles range of 5° – 90° , a step size of 0.01, and a scan speed of 2° min^{-1} . Characterization using Fourier transform infrared spectroscopy (FTIR) was undertaken to identify the unknown specimens and provide information on molecules' organic or inorganic nature. FTIR spectra were acquired on a PerkinElmer Spectrum GX FT-IR spectrometer. Initial Zn concentrations in ZnO NPs aqueous suspension were measured using an inductively coupled plasma atomic emission spectrometer (Agilent 5800 ICP-AES). The samples were digested using concentrated HNO_3 and then diluted to 5% HNO_3 before the analysis.

Stability and Zn release studies

A dissolution study was performed as described by Misra et al. (2011) by placing a portion of the nano form of

Zn-containing sunblock dispersed in water inside the interior of a dialysis tube (MWCO = 13.5 kDa) and transferring it to 250 mL plastic bottles (Nalgene) containing 200 mL of 1 mM $\text{Ca}(\text{NO}_3)_2$ (pH 7). In the current study, a relatively higher MW cut-off tube was used than Misra's (12.4 kDa), which was roughly estimated to be equivalent to a 1.2 nm pore size diameter. The starting ZnO content inside the dialysis tube was kept at 500 mg L^{-1} . The samples were incubated at 25°C in an end-over-end shaker. A proportion of 1 mL was taken from the medium outside the dialysis tube at regular intervals (from 0.5 to 98 h), acidified with 5% HNO_3 , and the Zn concentration was then measured using a triple quad inductively coupled plasma mass spectrometer (QQQ-ICP-MS, Agilent 8800, Tokyo, Japan).

Zn antimicrobial bioassay

The disc diffusion bioassay method (Akujobi and Njoku 2010; Hossain et al. 2022) was used to test the antibacterial activity of bulk ZnO and NPs at different concentrations. The soil sample used in the test was obtained from agricultural land in Rashid City, Behira Governorate, Egypt (location: $36.96^\circ 31' 23'' \text{ N}$, $20.80^\circ 30' 24'' \text{ W}$). The soil was classified as clay according to the FAO/USDA system, and it was characterized by sand, silt, and clay fractions of 30, 25, and 45%, respectively, and by pH moderately alkaline (pH 8.20).

Around 10 g of air-dried soil was added to 90 mL of distilled sterile water and shaken for 30 min. Another decimal dilution (10^{-2}) was prepared from the initial soil suspension, and further serial dilutions were undertaken till required (4th, 5th and 6th dilution). Soil water suspensions prepared from the fourth, fifth, and sixth dilution steps were plated into a Petri dish. Nutrient agar was used as a growing medium; aliquots of 1 mL of the soil suspensions at selected dilutions were injected into each sterile

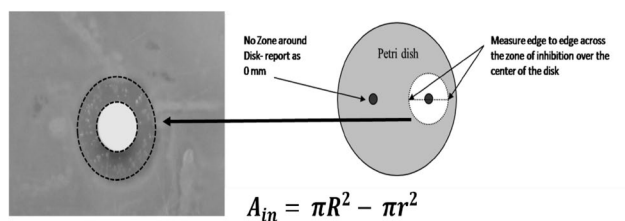


Fig. 2 Measurement method of the area of inhibition zone using disc diffusion methods according to Eq. 1

Petri dish. Then, 20 mL of pre-prepared molten nutrient agar was added. The plates were left to dry for about 3 min, and sterile paper discs (5 mm in diameter) were placed on their surface with different concentrations of different ZnO forms. Discs were soaked in a solution containing different concentrations of ZnO in different forms. Discs soaked in 20 μL of 70% ethanol served as a negative control. Augmentin[®], a commercial large-spectrum antibiotic containing amoxicillin and clavulanate as active ingredients, was used as a positive control. The inoculated plates were incubated at 30 °C for 4 days. Inhibition zone areas were measured around each disc with a scale as demonstrated in Fig. 2 using the formula:

$$A_{\text{in}} = \pi R^2 - \pi r^2, \quad (1)$$

where A_{in} = zone of inhibition $\pi = 3.1416$, R = inhibition zone radius, and r = original radius of the paper disc.

All tests were undertaken in triplicates. In detail, all forms and concentrations of samples tested in the bioassay study included: (1) ZnO in both forms of nanoparticles and pure bulk compounds at different concentrations (0, 0.5, 1.0, 5.0, and 10.0 mg L^{-1}); (2) water samples collected from the handwashing simulation experiment involving the four volunteers as described in "[ZnO NP-containing sunblock disposal route simulation](#)" (namely V1, V2, V3 and V4); (3) nano and non-nano-sized ZnO sunblocks (respectively, SunNP and SunBK for ZnO NPs and bulk ZnO containing sunblock) taken directly from the original containers and used at two different concentrations (50% and 100% which represent 9.0% and 18% of ZnO for both forms).

Statistical analysis

Each trial was conducted with three replicates except for the dissolution experiment, where two replicates were used to minimize the costs of ICP-MS analysis. The results were presented as arithmetic mean \pm standard deviation (SD). Paired t -test and Pearson correlation were undertaken using Minitab[®] 17.1.0 software.

Results and discussion

Characterizations of different forms of zinc oxide

SEM, TEM, and XRD characteristics

For their diameter and morphology, different techniques examined zinc oxide in different forms (ZnO NPs, ZnO bulk, SunBK, and SunNP). SEM presented a clear vision of the shape and size details of the ZnO NPs. The SEM demonstrated that the bulk ZnO particle size diameter ranged between 200 and 500 nm and that ZnO bulk exhibited a rocky surface and hexagonal shape, as clearly shown in Fig. 3. The particle diameter of ZnO NPs has estimated about 20–30 nm, as shown in Fig. 4. They displayed a uniform spherical shape instead.

The SEM image of SunBk and SunNP (Figs. 5, 6) confirmed that both ZnO forms were coated by sunblock's organic ingredients, which hindered the ZnO primary particle size distribution estimation.

The TEM imaging provided a clearer and more detailed insight into all the particles under scrutiny (Figs. 7, 8, 9). The nanoparticle size estimated from the TEM micrograph showed a size of less than 30 nm for ZnO NPs and SunNP. The TEM graph also validated that the zinc oxide nanoparticles were semi-spherical in shape and nearly uniform in size. The current results align with what was reported by Awasthi et al. (2017), which exhibited their ZnO NPs in an agglomerated state with almost spherical primary shapes. From the TEM image of non-nano sunblock (Fig. 9), it was also clear that ZnO size showed particle distribution with a primary size of more than 100 nm.

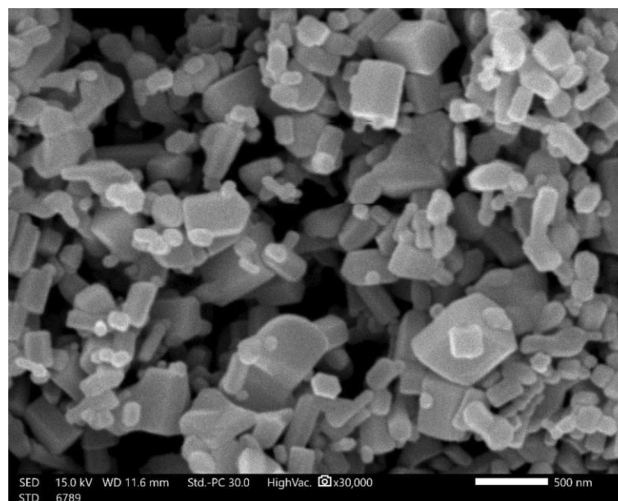


Fig. 3 SEM image of pure non-nano-form of zinc oxide (ZnO-Bulk)

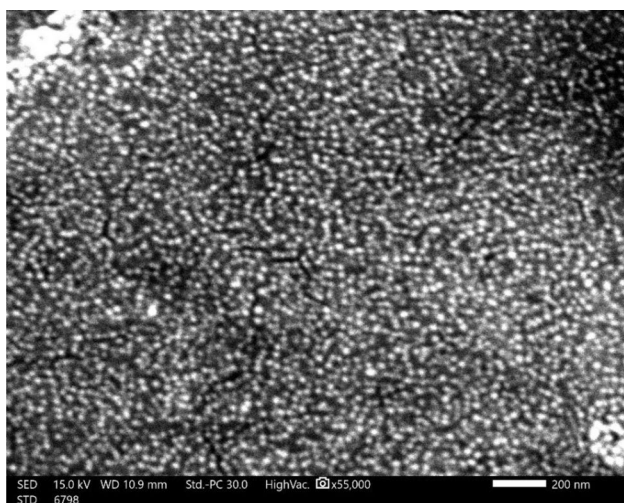


Fig. 4 SEM image of pure zinc oxide nanoparticles (ZnO NPs)

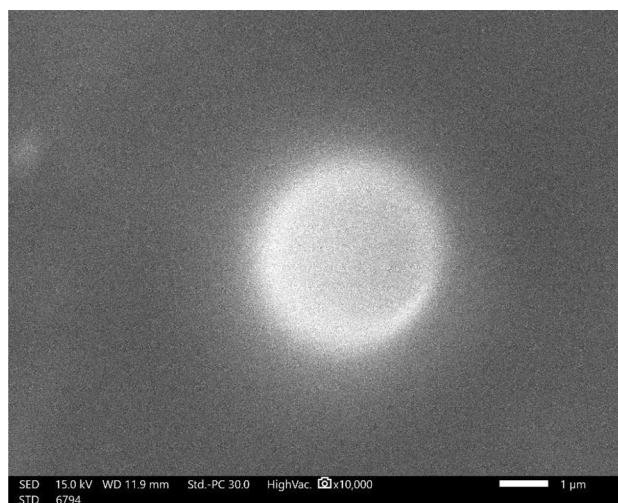


Fig. 6 SEM image of zinc oxide nanoparticles sunblock (SunNP)

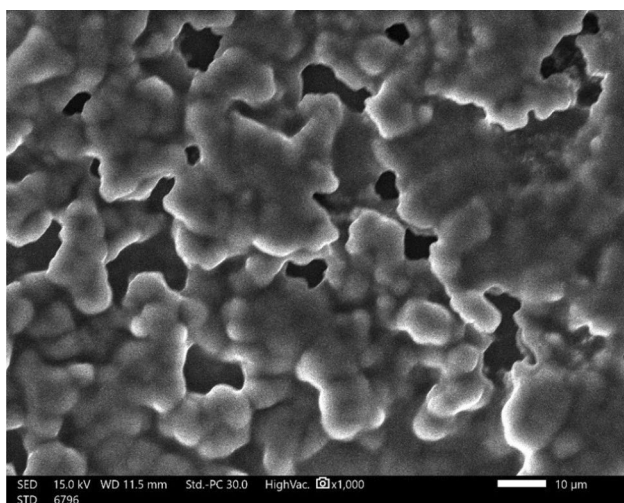


Fig. 5 SEM image of zinc oxide sunblock (SunBK)

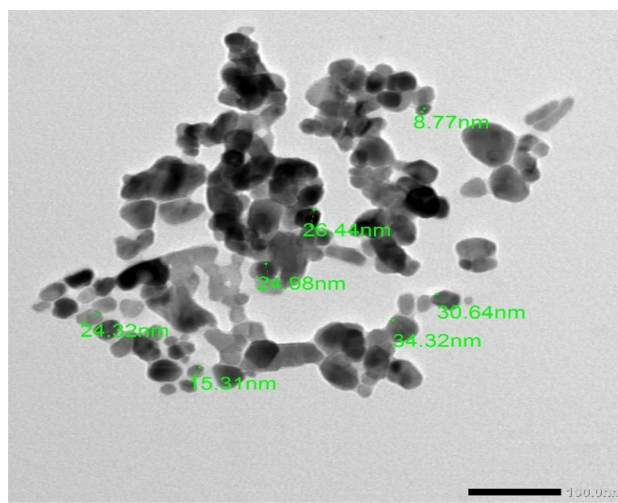


Fig. 7 TEM image of pure zinc oxide nanoparticles (ZnO NPs)

X-ray diffraction (XRD) patterns of ZnO NPs, SunBk, and SunNPs are shown in Fig. 10. All the powders have a similar XRD pattern, but the intensity levels are different. This is because of the random orientation of crystallographic planes (Tsutsumi et al. 2021). At 31.7° , 34.4° , 36.2° , 47.5° , 56.6° , 62.8° , 66.4° , 68.0° , and 77.0° , the diffraction peaks are obtained, which correspond to hexagonal ZnO structure with crystallographic (100), (002), (101), (102), (110), (103) (200), (112) and (202) directions as shown in Fig. 10 (Ladanov et al. 2011; Huang et al. 2001). Furthermore, the diffraction peak at 25.3° and 53.6° show the presence of TiO_2 in ZnO nanostructures-containing sunblock (Fig. 13, SunNP; matches with ICDD DB card no. 01-076-1939); in fact, TiO_2 is commonly used as an additive to improve sunblock efficacy in combination with ZnO nanostructures. The

results confirmed the presence of hexagonal phase ZnO with the ICDD card of ICSD 082028, which corresponded with both SEM and TEM findings.

To estimate the crystalline sizes of the ZnO NPs, the famous well-defined Scherrer equation ($D = (k\lambda/\beta_{hkl})\cos\theta$) was used. The crystalline sizes of the ZnO NPs, SunNPs, and SunBK were observed to be 149 nm, 2.72 nm, and 192 nm, respectively. This result demonstrated aggregation of ZnO NPs. Aggregation behavior of ZnO NPs could exist because the tiny particle has notably higher surface energy, and the development of particle attachment can minimize the free enthalpy of the system by lowering the surface area at a constant quantity. It has been reported by other studies that the bigger size of nanoparticles determined by different technology compared with TEM and XRD results is more

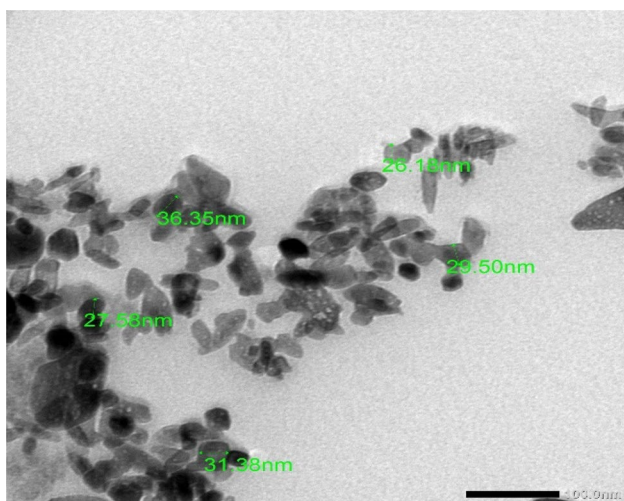


Fig. 8 TEM image of zinc oxide nanoparticles in sunblock (SunNPs)

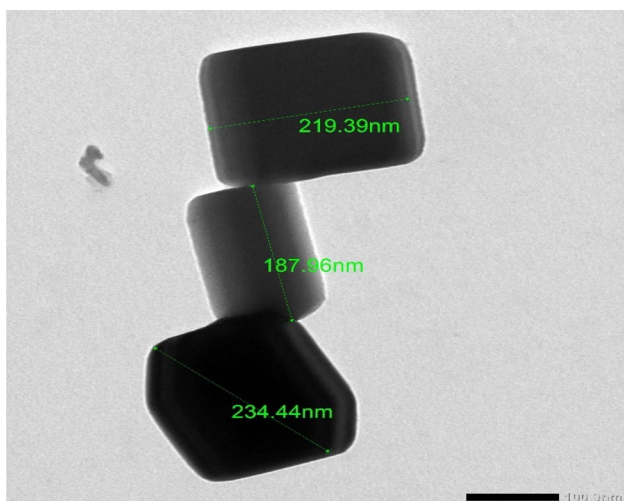


Fig. 9 TEM image of bulk zinc oxide in sunblock (SunBK)

likely due to the development of nano-metal oxide aggregates (Zhang 2003; Gericke and Pinches 2006). The actual environmental fate experiments and behavior of NPs generally focus on aggregation or agglomeration state and dispersion resulting from biological or environmental processes (Sekine et al. 2017). However, the size of ZnO in sunblock appears reasonably and relatively consistent as the sunblock cream behaves as a stabilizer agent to maintain ZnO in its original size.

FTIR and UV–Vis

FTIR spectroscopy was performed to determine the functional groups in ZnO powders. Figure 11 shows the FTIR spectrum of different ZnO forms with wave range from

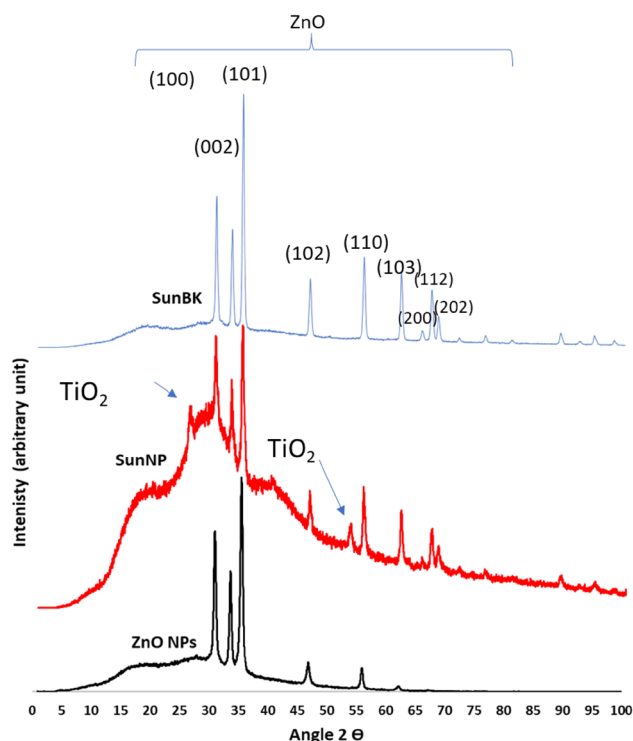


Fig. 10 The XRD pattern of ZnO nanoparticle (ZnO NPs), ZnO NPs-containing sunblock (SunNP), and ZnO bulk-containing sunblock (SunBK)

4000 to 500 cm^{-1} . As shown in Fig. 11, all spectrums showed the same trend; the same component is dominant with some exceptions. The broad typical band of IR spectroscopy at 2900–3000 is due to absorbed H_2O (OH bond stretching). Moreover, the peaks in this region (2900–3000) may be due to C–H stretching of organic impurities in the Sun-NP and Sun-BK. The peak at 3450 cm^{-1} correlates to OH presence due to atmospheric moisture absorbed onto the surface of ZnO nanostructures (Anžlovar et al. 2012). The stretch peak around 400 to 500 for SunNP could represent the impurity of ZnO NPs due to the existence of TiO_2 in the sunblock cream used in the current study, as shown in the XRD results in Fig. 10. The peaks between 1600.00 and 600.93 cm^{-1} correspond to ZnO stretching and deformation vibration, respectively. These results were similar to FTIR spectra observed by Kumar and Rani (2013).

UV–Visible absorption spectrum of synthesized nanoparticles for SunBK and SunNP is shown in Fig. 12. The distinct peak centered around 300 nm is specific for ZnO NPs immersed in sunblock (SunNP) due to their multiple excitation binding energy at room temperature (Bhuyan et al. 2015). The disappearance of this peak in the case of SunBK can be due to a high increase in particle size (Fakhari et al. 2019).

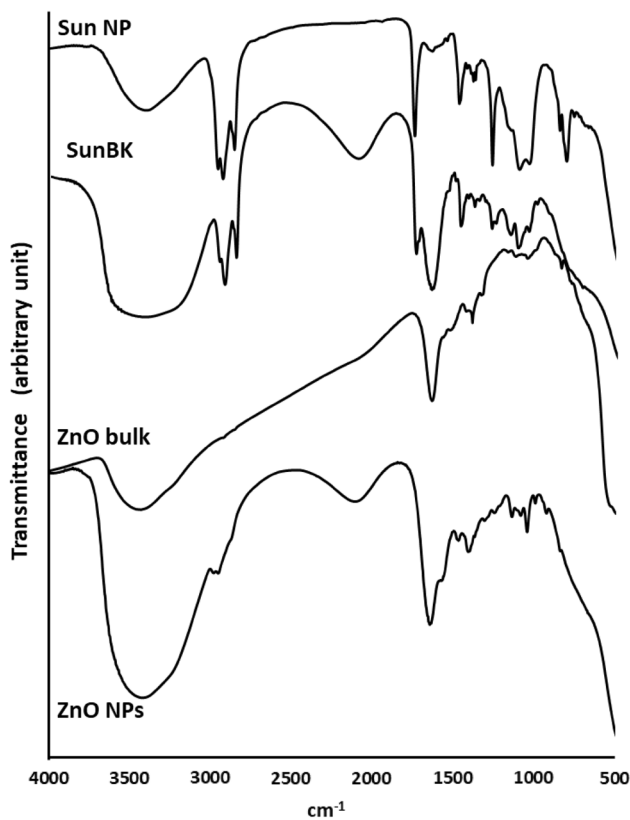


Fig. 11 FTIR Spectra of the different ZnO forms under scrutiny

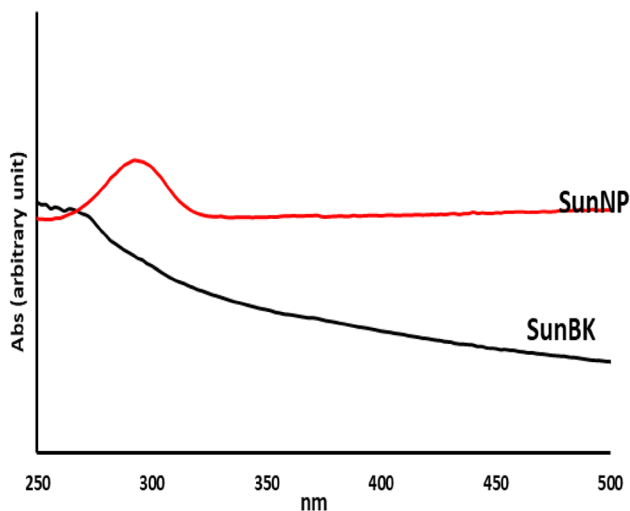


Fig. 12 UV–Visible spectrum of SunNP and SunBK

ICP-AES and EDX

The ICP-AES results showed that the total Zn concentrations in the water disposed of during the hand washing test involving the four volunteers were 0.20, 0.23, 0.21, and 0.34 mg L⁻¹ for V1, V2, V3, and V4, respectively.

The EDX confirmed that the significant element identified in all measured materials was ZnO but that also TiO₂ was identified in the SunNPs product. The ZnO percentage obtained from the EDX results was 98.2 ± 1.74% for the bulk ZnO, 82.3 ± 1.45% for the ZnO NPs, and 45.7 ± 0.96% for the SunBK. For the SunNPs sunblock, the ZnO and the TiO₂ amounts were, respectively, 3.80 ± 0.29% and 1.81 ± 0.10%.

Zinc oxide nanoparticle dissolution study

This experiment aimed to study the chemical stability of engineered ZnO nanoparticles in soil water. Since the release of an element from its analog NPs could be primarily influenced by water chemistry composition (Van der Vliet and Ritz 2013; Sharon et al. 2010), the ZnO NPs stability/dissolution study was undertaken in 0.01 M Ca(NO₃)₂ that is considered as a good proxy standard for soil solution (Degryse et al. 2011; Marzouk et al. 2013). Table 1 shows Zn concentrations dissolved from the ZnO NPs as a function of time. The results showed that the Zn dissociated from NPs increased by increasing the incubation time, although the estimated dissolution was very small. In this regard, the amount of Zn ions dissociated from NPs, as a proportion of the total ZnO NPs addition, increased from 0.017% after 30 min to 0.47% at 98 h.

The dissolution of ZnO NPs is a complicated process that a simple mathematical model cannot express. The modified first-order kinetics model (Eq. 2), as described by van de Venter (2001), Halliwell and Gutteridge (1984), has been used to describe these data.

Table 1 Zinc concentration (µg L⁻¹) measured in the Ca-nitrate electrolyte as a result of ZnO NPs dissolution outside the dialysis tube as a function of time (hours)

Time (h)	Average Zn concentration (µg L ⁻¹)	Standard deviation (µg L ⁻¹)
0.5	85.4	0.52
1	352	2.27
2	725	9.16
4	1313	5.35
6	1613	1.36
8	1973	10.6
10	2132	9.49
12	2272	25.0
24	2357	291
36	2333	40.8
48	2360	19.4
72	2352	246
98	2478	304

$$Y_t = (Y_{\text{final}}(1 - \exp^{-kt})), \quad (2)$$

where Y_t is the dissolved ZnO NPs ($\mu\text{g L}^{-1}$ Zn) at the time t (h), Y_{final} is the final solubility, and k is the dissolution rate coefficient (h^{-1}). This equation has been selected as it describes the growth rate of Zn outside the dialysis tube. It was primarily used to describe organism growth or mortality as a function of time. However, it will describe the kinetic reaction of the current study as demonstrated by Halliwell and Gutteridge (1984).

The estimated k and Y_{final} values for Zn were $0.176 \mu\text{g L}^{-1} \text{h}^{-1}$ and $2478 \mu\text{g L}^{-1}$, respectively, indicating low dissolution impacts on the kinetics and steady-state solubility of ZnO NPs under the Ca-nitrate condition. This test estimated a high R^2 value (0.97), which suggests that the proposed model could well describe the kinetics of zinc dissolution, as shown in both Figs. 13 and 14. Nevertheless, Eq. 2 slightly overestimates the Zn solubility throughout equilibration times, and the general average predicted from the proposed model ($1744 \mu\text{g L}^{-1}$) was relatively higher than the solubility determined after 98 h ($1718 \mu\text{g L}^{-1}$) although still in a reasonable range (Figs. 13, 14). It should be remarked that this kind of mathematical model is an algebraic simplification of the occurring phenomenon like any other similar model, based on a few variables that do not consider all the specific mechanistic processes and the related consequences. To try to achieve better performances, other variables, such as the exact shape, size, and chemical composition of nanoparticles and interactions with their released free ions and physico-chemical characteristics of the organics added, should/could be included in the proposed model (Assche and Clijsters 1990). However, it should also be stressed that the increase

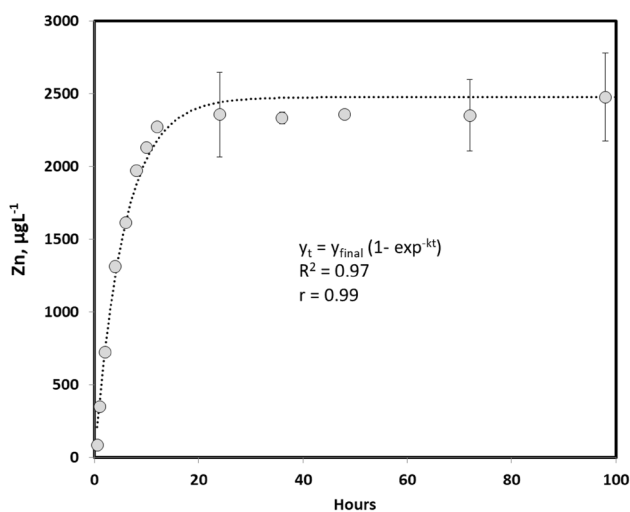


Fig. 13 Dissolution kinetics of ZnO NPs in 0.01 M $\text{Ca}(\text{NO}_3)_2$. The data were fitted to a modified first-order reaction equation. Error bars represent standard deviations ($n=2$)

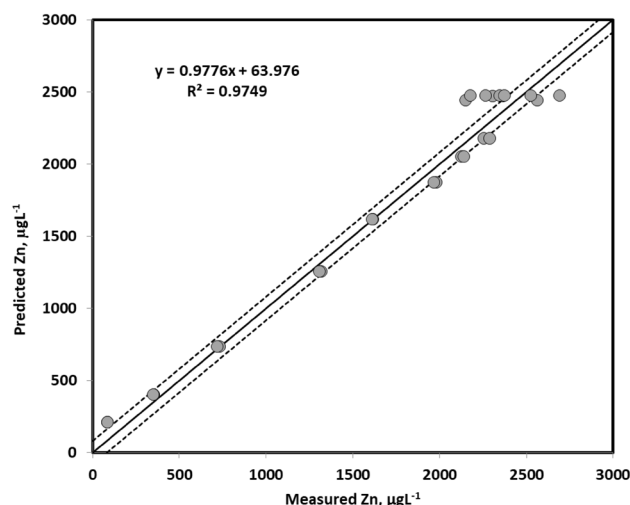


Fig. 14 Predicted against measured values of Zn dissociated from ZnO NPs as described by Eq. 2. The solid line represents a 1: 1 relationship while broken lines represent 1 RSD value [residual standard deviation, the model error (Meharg 1994)]. The plotted points represent all the individual replicates instead of the average values

in model complexity does not often produce the expected improvements in performance and accuracy.

Because the dissolution rate of the nanomaterial needs to be considered to explain the results and, more importantly, design experiments, the benefit of the dissolution experiment is very important in monitoring the toxicity and bioaccumulation of nanoparticulated systems. As a result, this work could not have been completed without first studying the rate at which ZnO NPs dissolve.

Disc diffusion bioassay

Effect of pure materials

In the present investigation, soil bacteria were used to investigate the antimicrobial properties of different forms of Zn using disc diffusion bioassay (DDB). Different forms of ZnO demonstrated high antimicrobial activity and displayed a large inhibition zone area. The 10 mg L^{-1} Zn concentration showed the highest inhibition zone compared with other treatments. Figures 15 and 16 show that the area of the inhibition zone increased with the increasing Zn concentrations for both treatments (pure ZnO nanoparticles and pure bulk forms).

The highest inhibition zone was detected at the highest Zn concentrations (10 mg L^{-1}), with 82.9 and 67.6 mm^2 for pure ZnO NPs and bulk, respectively. Likewise, the lowest inhibition was paralleled with the lowest Zn concentrations (0.5 mg L^{-1}) with values of 25.9 and 35.4 mm^2 for pure ZnO NPs and bulk, respectively. Figure 17 shows that with all ZnO concentrations, the inhibition zone area showed one

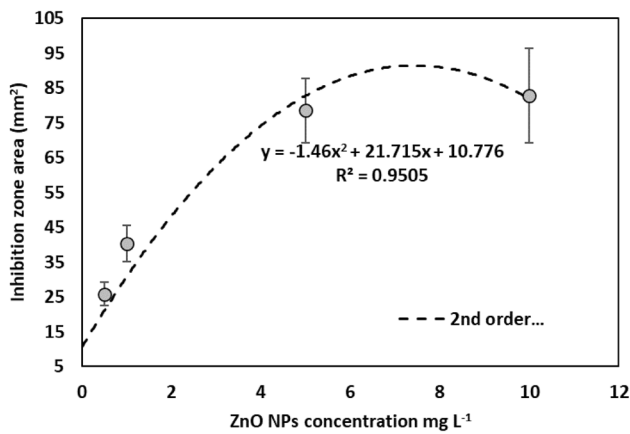


Fig. 15 Effect of different ZnO NPs concentrations on the inhibition zone area for soil bacteria using the disc diffusion bioassay. Error bars represent standard deviations ($n=9$)

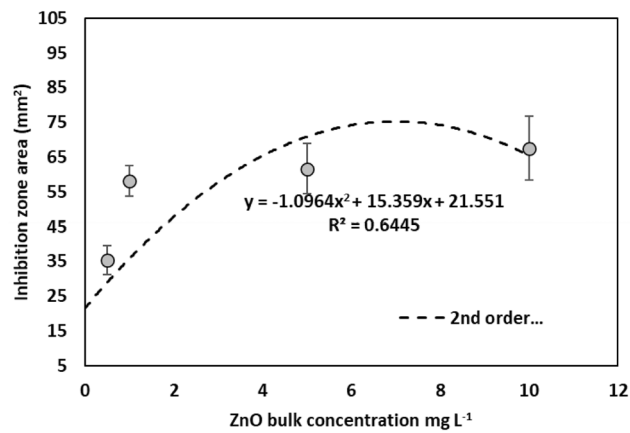


Fig. 16 Effect of different bulk ZnO concentrations on inhibition zone area for soil bacteria using disc diffusion bioassay. Error bars represent standard deviations ($n=9$)

order of magnitude smaller compared with the effect of the positive control (Augmentin antibiotic). The effects of bulk ZnO are dominant at lower concentrations, up to 1 mg L^{-1} . Compared with a concentration higher than 1 mg L^{-1} of ZnO, the nanosized ZnO showed more inhibition zone area than bulk size (Fig. 17). This result indicates a larger antimicrobial activity influence due to the nano-specificity at higher concentrations only. Raghupathi et al. (2011) used different particle sizes of ZnO and studied their impact on bacteria. They found that antibacterial activity increased with decreasing particle size from approximately 200 to 10 nm. The authors found that with a particle size of ZnO of more than 100 nm, the toxicity of methicillin-sensitive *S. aureus* was inadequate. It seemed that the bacteriostatic function of ZnO NPs was a phenomenon occurring where the NPs size is smaller than the diameter of the bulk form (Figs. 3, 4).

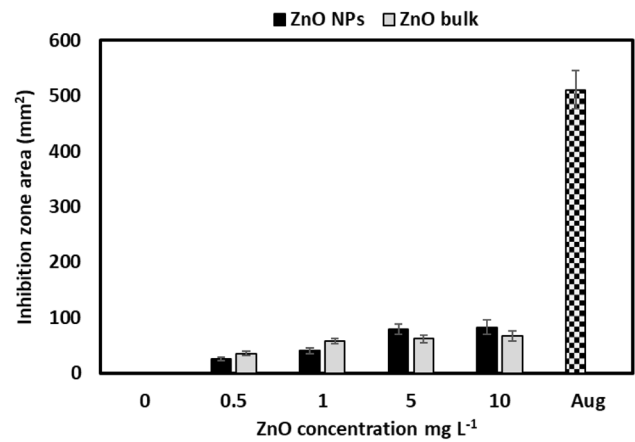


Fig. 17 Inhibition zone area (mm^2) as affected by pure ZnO (both nano and bulk size) at different concentrations; 0.0, 0.5, 1, 5, and 10 mg L^{-1} . Augmentin, a commercial antibiotic, was included as a reference line (Aug). Error bars represent standard deviations ($n=9$ for each ZnO concentration and $n=3$ for Aug)

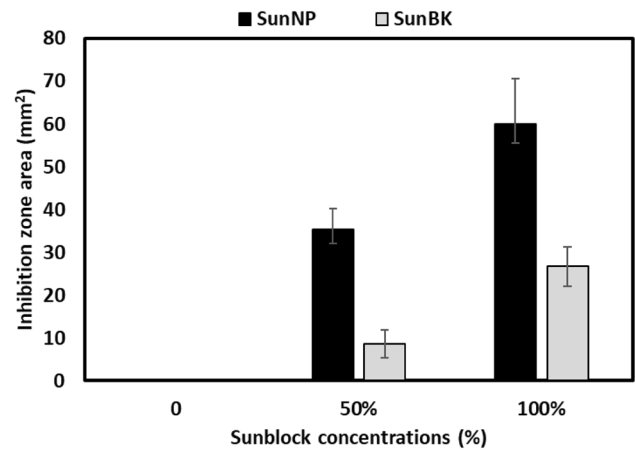


Fig. 18 Inhibition zone area (mm^2) of both nano and bulk sunblock types at different concentrations (0, 50, and 100% of the commercial product, i.e., 0.0, 9.0, and 18% of ZnO). Error bars represent standard deviations ($n=9$)

A correlation test was run between the inhibition zone area and the Zn concentration. A positive correlation was observed only in the case of the nanoparticle treatment ($R^2=0.88$, $p<0.05$ for ZnO NPs while $R^2=0.69$, $p>0.05$ for bulk ZnO). Furthermore, a t -paired test showed that although there was a difference between the effects of ZnO NP and bulk forms on the inhibition zone area, it was not a significant difference ($t=015$, $p=0.89$). It has been reported that the toxicity effect of ZnO NPs is comparable to the concentration level of NPs (Liu et al. 2009b; Janaki et al. 2015; da Silva et al. 2019).

In an attempt to show the direct effects of sunblock cream on the inhibition zone area, Fig. 18 reported the effect of

SunNP and SunBK at 50% and 100% of the initial concentration in the cream. The results showed that the effect of pure sunblock containing nano-size ZnO was more toxic than the bulk-size ZnO form. The inhibition zone area increased with the sunblock ZnO concentration in both forms (ZnO NP; $R^2 = 0.99$, $p < 0.01$, ZnOBK; $R^2 = 0.95$, $p < 0.01$).

According to previous studies, different pathogenic bacteria (such as *Salmonella* spp., *Staphylococcus aureus*, *Listeria monocytogenes*, and *Escherichia coli*) have been monitored under ZnO NPs applications (Applerot et al. 2009; Jin et al. 2009; Liu et al. 2009b; Menazea et al. 2021) with variable toxicity outcome. According to these published results, it might be hypothesized that particle size and specific bacterial sensitivity could be relevant among the various factors controlling toxicity. Three criteria could be used to manage the toxicity level of ZnO NPs to microorganisms: (1) dissolution kinetic of ZnO NPs, (2) promotion of ROS generation, (3) immediate contact with biologic targets, and (4) environmental conditions (Book and Backhaus 2022; Liu et al. 2022; Li et al. 2011).

Effect of disposed water from handwashing trial

The handwashing trial performed in the current study was aimed to simulate and model the potential effects on the ZnO NPs during the route into the WWTP. Figure 19 showed that the effects recorded in these tests were similar to those in the pure materials. There was a significant increase in inhibition zone area (IZA) with increased Zn concentrations in the disposed washing solution (DWS). Pearson correlation coefficient between Zn content in DWS and IZA was 0.86 with a p -value < 0.01 . The highest IZA was observed with the highest Zn content in DWS, 8.45 mm² with 0.34 mg L⁻¹ (Fig. 20). The interaction between ZnO NP-DWS and soil microorganisms was significantly negative. In addition, it

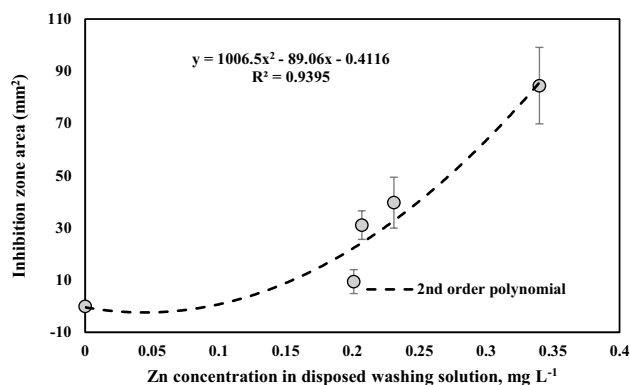


Fig. 19 Relationship between inhibition zone area (mm²) and Zn concentration in the disposed of washing solution obtained from the SunNP applied to the human skin. Error bars represent standard deviations ($n = 9$)

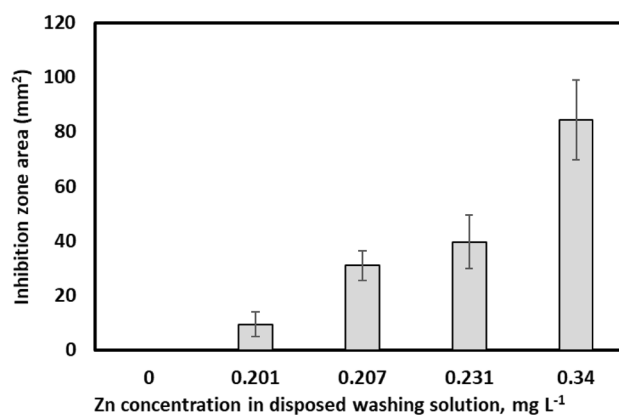


Fig. 20 Effect on Inhibition zone area (mm²) of different concentrations of SunNP from the disposed of washing solution. Error bars represent standard deviations ($n = 9$)

should be considered that other factors apart from the nanoparticles may as well contribute to the toxicity. Sunblocks usually contain other ingredients and different coating materials to improve the ZnO NPs stability. For example, it has been reported that the organosilanes coating process could change the surface of ZnO NPs to increase the sunblock formula's stability (Chen and Yakovlev 2010). Therefore, the higher toxicity of soil microorganisms from the sunblock-derived ZnO NPs might be explained by the additional effects of the coating materials and other additives in the preparation.

Conclusion

This work aimed to investigate the impact of zinc oxide nanoparticles (ZnO NPs) present in sunblock cosmetics on soil microorganisms. We found that the toxic effect of pure sunblock containing nano ZnO on soil microbes is higher than bulk ZnO. The toxicity effect of sunblock ZnO NPs might be driven by some coating materials added to the nanoparticles and other co-formulants. Our work provides valuable information on the impact of ZnO NPs on soil microorganisms. This is mainly because previous studies have mainly focused on the effects of bulk ZnO on isolated organisms rather than investigating the impact on real environmental studies. However, this study examines the influence of ZnO NPs, specifically in sunblock products, on soil microorganisms. Future research should further elucidate the mechanisms by which ZnO NPs impact soil microorganisms and the larger soil ecosystem. Additionally, studies should aim to compare the toxicity of different ZnO NPs under controlled conditions to understand better the impact of particle size, shape, coating materials, and co-formulants on toxicity. Further research on the transport and fate of ZnO NPs in the environment would

also be valuable in understanding their potential ecological impacts.

Acknowledgements The authors are thankful to Dr. Eman Abdalla, Ms. Tahany Kamal, Mr. Saed Allam, and Ms. Nermen Mohamed, who agreed to participate as volunteers in the study.

Author contributions EA and EM conceived the research idea. EA and EM designed the research. EA and EM conducted experiments at Arish University. GB provided pure nanoparticle materials from Australia. EM and WS analyzed data. EM wrote the original draft. All authors reviewed, edited, and approved the manuscript.

Funding Open access funding provided by The Science, Technology & Innovation Funding Authority (STDF) in cooperation with The Egyptian Knowledge Bank (EKB).

Data availability The dataset used in the study will be made available by the corresponding author upon reasonable request.

Declarations

Conflict of interest Authors declare no competing interest.

Ethics approval and consent to participate Informed consent was obtained from all individual participants included in the study.

Consent for publication Consent for publication was obtained from all individual participants included in the study.

Open Access This article is licensed under a Creative Commons Attribution 4.0 International License, which permits use, sharing, adaptation, distribution and reproduction in any medium or format, as long as you give appropriate credit to the original author(s) and the source, provide a link to the Creative Commons licence, and indicate if changes were made. The images or other third party material in this article are included in the article's Creative Commons licence, unless indicated otherwise in a credit line to the material. If material is not included in the article's Creative Commons licence and your intended use is not permitted by statutory regulation or exceeds the permitted use, you will need to obtain permission directly from the copyright holder. To view a copy of this licence, visit <http://creativecommons.org/licenses/by/4.0/>.

References

- Adams LK, Lyon DY, Alvarez PJ (2006) Comparative eco-toxicity of nanoscale TiO₂, SiO₂, and ZnO water suspensions. *Water Res* 40:3527–3532
- Akujobi C, Njoku H (2010) Bioassay for the determination of microbial sensitivity to Nigerian honey. *Glob J Pharmacol* 4:36–40
- Anžlovar A, Orel ZC, Kogej K, Žigon M (2012) Polyol-mediated synthesis of zinc oxide nanorods and nanocomposites with poly (methyl methacrylate). *J Nanomater* 2012:760872
- Applerot G, Lipovsky A, Dror R, Perkash N, Nitzan Y, Lubart R, Gedanken A (2009) Enhanced antibacterial activity of nanocrystalline ZnO due to increased ROS-mediated cell injury. *Adv Func Mater* 19:842–852
- Aruoja V, Dubourguier H-C, Kasemets K, Kahru A (2009) Toxicity of nanoparticles of CuO, ZnO and TiO₂ to microalgae *Pseudokirchneriella subcapitata*. *Sci Total Environ* 407:1461–1468
- Assche FV, Clijsters H (1990) Effects of metals on enzyme activity in plants. *Plant Cell Environ* 13:195–206
- Awasthi A, Bansal S, Jangir LK, Awasthi G, Awasthi KK, Awasthi K (2017) Effect of ZnO nanoparticles on germination of *Triticum aestivum* seeds. *Macromolecular symposia*, 2017. Wiley Online Library, p 1700043
- Bhuyan T, Mishra K, Khanuja M, Prasad R, Varma A (2015) Biosynthesis of zinc oxide nanoparticles from *Azadirachta indica* for antibacterial and photocatalytic applications. *Mater Sci Semicond Process* 32:55–61
- Book F, Backhaus T (2022) Aquatic ecotoxicity of manufactured silica nanoparticles: a systematic review and meta-analysis. *Sci Total Environ* 806:150893
- Chen Q, Yakovlev NL (2010) Adsorption and interaction of organosilanes on TiO₂ nanoparticles. *Appl Surf Sci* 257:1395–1400
- da Silva BL, Abuçafy MP, Manaia EB, Junior JAO, Chiari-Andréo BG, Pietro RCR, Chiavacci LA (2019) Relationship between structure and antimicrobial activity of zinc oxide nanoparticles: an overview. *Int J Nanomed* 14:9395
- Degryse F, Voegelin A, Jacquat O, Kretzschmar R, Smolders E (2011) Characterization of zinc in contaminated soils: complementary insights from isotopic exchange, batch extractions and XAFS spectroscopy. *Eur J Soil Sci* 62:318–330
- Duan X, Zhou X, Wang R, Wang S, Ren N-Q, Ho S-H (2021) Advanced oxidation processes for water disinfection: features, mechanisms and prospects. *Chem Eng J* 409:128207
- Fajardo C, Martinez-Rodriguez G, Blasco J, Mancera JM, Thomas B, de Donato M (2022) Nanotechnology in aquaculture: applications, perspectives and regulatory challenges. *Aquac Fish* 7:185–200
- Fakhari S, Jamzad M, Kabiri Fard H (2019) Green synthesis of zinc oxide nanoparticles: a comparison. *Green Chem Lett Rev* 12:19–24
- Ferreira T, Rasband W (2012) ImageJ user guide. *ImageJ/Fiji* 1:155–161
- Gelover S, Gómez LA, Reyes K, Leal MT (2006) A practical demonstration of water disinfection using TiO₂ films and sunlight. *Water Res* 40:3274–3280
- Gericke M, Pinches A (2006) Biological synthesis of metal nanoparticles. *Hydrometallurgy* 83:132–140
- Hajipour MJ, Fromm KM, Ashkarran AA, de Aberasturi DJ, de Larremendi IR, Rojo T, Serpooshan V, Parak WJ, Mahmoudi M (2012) Antibacterial properties of nanoparticles. *Trends Biotechnol* 30:499–511
- Halliwell B, Gutteridge J (1984) Oxygen toxicity, oxygen radicals, transition metals and disease. *Biochem J* 219:1
- Heinlaan M, Ivask A, Blinova I, Dubourguier H-C, Kahru A (2008) Toxicity of nanosized and bulk ZnO, CuO and TiO₂ to bacteria *Vibrio fischeri* and crustaceans *Daphnia magna* and *Thamnocephalus platyurus*. *Chemosphere* 71:1308–1316
- Hossain ML, Lim LY, Hammer K, Hettiarachchi D, Locher C (2022) A review of commonly used methodologies for assessing the antibacterial activity of honey and honey products. *Antibiotics* 11:975
- Huang MH, Wu Y, Feick H, Tran N, Weber E, Yang P (2001) Catalytic growth of zinc oxide nanowires by vapor transport. *Adv Mater* 13:113–116
- Hurley RR, Nizzetto L (2018) Fate and occurrence of micro (nano) plastics in soils: knowledge gaps and possible risks. *Curr Opin Environ Sci Health* 1:6–11
- Ibrahim AS, Ali GAM, Hassanein A, Attia AM, Marzouk ER (2022) Toxicity and uptake of CuO nanoparticles: evaluation of an emerging nanofertilizer on wheat (*Triticum aestivum* L.) plant. *Sustainability* 14:4914
- Janaki AC, Sailatha E, Gunasekaran S (2015) Synthesis, characteristics and antimicrobial activity of ZnO nanoparticles. *Spectrochim Acta Part A Mol Biomol Spectrosc* 144:17–22

- Jiang W, Mashayekhi H, Xing B (2009) Bacterial toxicity comparison between nano- and micro-scaled oxide particles. *Environ Pollut* 157:1619–1625
- Jin T, Sun D, Su J, Zhang H, Sue HJ (2009) Antimicrobial efficacy of zinc oxide quantum dots against *Listeria monocytogenes*, *Salmonella enteritidis*, and *Escherichia coli* O157: H7. *J Food Sci* 74:M46–M52
- Kołodziejczak-Radzimska A, Jesionowski T (2014) Zinc oxide—from synthesis to application: a review. *Materials* 7:2833–2881
- Kubo M, Onodera R, Shibasaki-Kitakawa N, Tsumoto K, Yonemoto T (2005) Kinetics of ultrasonic disinfection of *Escherichia coli* in the presence of titanium dioxide particles. *Biotechnol Prog* 21:897–901
- Kumar H, Rani R (2013) Structural and optical characterization of ZnO nanoparticles synthesized by microemulsion route. *Int Lett Chem Phys Astron* 14:26–36
- Kumar A, Kaur K, Sharma S (2013) Synthesis, characterization and antibacterial potential of silver nanoparticles by *Morus nigra* leaf extract. *Indian J Pharm Biol Res* 1:16–24
- Ladanov M, Ram M, Kumar A, Matthews G (2011) Novel aster-like ZnO nanowire clusters for nanocomposites. MRS online proceedings library (OPL), p 1312
- Li Z, Greden K, Alvarez PJ, Gregory KB, Lowry GV (2010) Adsorbed polymer and NOM limits adhesion and toxicity of nano scale zerovalent iron to *E. coli*. *Environ Sci Technol* 44:3462–3467
- Li M, Zhu L, Lin D (2011) Toxicity of ZnO nanoparticles to *Escherichia coli*: mechanism and the influence of medium components. *Environ Sci Technol* 45:1977–1983
- Liu B, Li X, Li B, Xu B, Zhao Y (2009a) Carbon nanotube based artificial water channel protein: membrane perturbation and water transportation. *Nano Lett* 9:1386–1394
- Liu Y-J, He L-L, Mustapha A, Li H, Hu Z, Lin M-S (2009b) Antibacterial activities of zinc oxide nanoparticles against *Escherichia coli* O157: H7. *J Appl Microbiol* 107:1193–1201
- Liu J, Chen X, Shu H-Y, Lin X-R, Zhou Q-X, Bramryd T, Shu W-S, Huang L-N (2018) Microbial community structure and function in sediments from e-waste contaminated rivers at Guiyu area of China. *Environ Pollut* 235:171–179
- Liu Y, Zhu S, Gu Z, Chen C, Zhao Y (2022) Toxicity of manufactured nanomaterials. *Particuology* 69:31–48
- Lovrić J, Cho SJ, Winnik FM, Maysinger D (2005) Unmodified cadmium telluride quantum dots induce reactive oxygen species formation leading to multiple organelle damage and cell death. *Chem Biol* 12:1227–1234
- Madkhali OA, Sivagurunathan Moni S, Sultan MH, Bukhary HA, Ghazwani M, Alhakamy NA, Meraya AM, Alshahrani S, Alqahtani SS, Bakkari MA (2021) Formulation and evaluation of injectable dextran sulfate sodium nanoparticles as a potent antibacterial agent. *Sci Rep* 11:1–12
- Malhotra SPK, Mandal T (2019) Zinc oxide nanostructure and its application as agricultural and industrial material. *Contam Agric Environ Health Risks Remediat* 1:216
- Marzouk ER, Chenery SR, Young SD (2013) Predicting the solubility and lability of Zn, Cd, and Pb in soils from a minespoil-contaminated catchment by stable isotopic exchange. *Geochim Cosmochim Acta* 123:1–16
- Mayor DJ, Gray NB, Elver-Evans J, Midwood AJ, Thornton B (2013) Metal-macrofauna interactions determine microbial community structure and function in copper contaminated sediments. *PLoS ONE* 8:e64940
- Mbonyiriyivuze A, Zongo S, Diallo A, Bertrand S, Minani E, Yadav LL, Mwakikunga BW, Dhlamini SM, Maaza M (2015) Titanium dioxide nanoparticles biosynthesis for dye sensitized solar cells application. review. *Phys Mater Chem* 3(1):12–17
- Mcintyre RA (1994) Integrated tolerance mechanisms: constitutive and adaptive plant responses to elevated metal concentrations in the environment. *Plant Cell Environ* 17:989–993
- Mcintyre RA (2012) Common nanomaterials and their use in real world applications. *Sci Prog* 95:1–22
- Menazea A, Ismail A, Samy A (2021) Novel green synthesis of zinc oxide nanoparticles using orange waste and its thermal and antibacterial activity. *J Inorg Organomet Polym Mater* 31:4250–4259
- Mileyeva-Biebesheimer ON, Zaky A, Gruden CL (2010) Assessing the impact of titanium dioxide and zinc oxide nanoparticles on bacteria using a fluorescent-based cell membrane integrity assay. *Environ Eng Sci* 27:329–335
- Misra SK, Dybowska A, Berhanu D, Croteau MNL, Luoma SN, Boccaccini AR, Valsami-Jones E (2011) Isotopically modified nanoparticles for enhanced detection in bioaccumulation studies. *Environ Sci Technol* 46:1216–1222
- Nagarajan R (2008) Nanoparticles: building blocks for nanotechnology. ACS Publications, Washington, D.C.
- Neal AL (2008) What can be inferred from bacterium–nanoparticle interactions about the potential consequences of environmental exposure to nanoparticles? *Ecotoxicology* 17:362–371
- Niazi JH, Gu MB (2009) Toxicity of metallic nanoparticles in microorganisms—a review. In: Kim YJ, Platt U, Gu MB, Iwahashi, H (eds) Atmospheric and biological environmental monitoring. Springer Netherlands, Dordrecht, pp 193–206
- Pacitto A, Stabile L, Morawska L, Nyarku M, Torkmahalleh MA, Akhmetvaliyeva Z, Andrade A, Dominski FH, Mantecca P, Shetaya WH, Mazaheri M, Jayaratne R, Marchetti S, Hassan SK, El-Mekawy A, Mohamed EF, Canale L, Frattolillo A, Buonanno G (2021) Daily submicron particle doses received by populations living in different low- and middle-income countries. *Environ Pollut* 269:116229
- Raghupathi KR, Koodali RT, Manna AC (2011) Size-dependent bacterial growth inhibition and mechanism of antibacterial activity of zinc oxide nanoparticles. *Langmuir* 27:4020–4028
- Santos-Rasera JR, Monteiro RTR, De Carvalho HWP (2022) Investigation of acute toxicity, accumulation, and depuration of ZnO nanoparticles in *Daphnia magna*. *Sci Total Environ* 821:153307
- Sekine R, Marzouk ER, Khaksar M, Scheckel KG, Stegemeier JP, Lowry GV, Donner E, Lombi E (2017) Aging of dissolved copper and copper-based nanoparticles in five different soils: short-term kinetics vs. long-term fate. *J Environ Qual* 46(6):1198–1205
- Sharon M, Choudhary AK, Kumar R (2010) Nanotechnology in agricultural diseases and food safety. *J Phyto* 2(4):83–92
- Smijs TG, Pavel S (2011) Titanium dioxide and zinc oxide nanoparticles in sunscreens: focus on their safety and effectiveness. *Nanotechnol Sci Appl* 4:95
- Sungur Ş (2021) Titanium dioxide nanoparticles. In: Handbook of nanomaterials and nanocomposites for energy and environmental applications, Springer International Publishing, Cham, pp 713–730
- Tsutsumi Y, Ishimoto T, Oishi T, Manaka T, Chen P, Ashida M, Doi K, Katayama H, Hanawa T, Nakano T (2021) Crystallographic texture-and grain boundary density-independent improvement of corrosion resistance in austenitic 316L stainless steel fabricated via laser powder bed fusion. *Addit Manuf* 45:102066
- van der Venter A (2001) Seed vigor testing. *J New Seeds* 2:51–58
- van der Vliet L, Ritz C (2013) Statistics for analyzing ecotoxicity test data. In: Férard J-F, Blaise C (eds) Encyclopedia of aquatic ecotoxicology. Springer, Dordrecht
- Wu K, Liu J, Chugh VK, Liang S, Saha R, Krishna VD, Cheeran MC, Wang J-P (2022) Magnetic nanoparticles and magnetic particle spectroscopy-based bioassays: a 15-year recap. *Nano Futures* 6:022001

- Xie Y, Wang J, Wu Y, Ren C, Song C, Yang J, Yu H, Giesy JP, Zhang X (2016) Using in situ bacterial communities to monitor contaminants in river sediments. *Environ Pollut* 212:348–357
- Zhang S (2003) Fabrication of novel biomaterials through molecular self-assembly. *Nat Biotechnol* 21:1171
- Zhao Q, Li X, Xiao S, Peng W, Fan W (2021) Integrated remediation of sulfate reducing bacteria and nano zero valent iron on cadmium contaminated sediments. *J Hazard Mater* 406:124680

Publisher's Note Springer Nature remains neutral with regard to jurisdictional claims in published maps and institutional affiliations.